JOURNAL OF MATERIALS SCIENCE 18 (1983) 1381–1388

Thermally activated crystallization of $(GeSe_2)_{70}$ $(Sb_2Te_3)_{20}(GeTe)_{10}$ alloy glass: morphological and calorimetric study*

M. T. CLAVAGUERA-MORA, S. SURIÑACH, M. D. BARÓ, N. CLAVAGUERA‡
Departamento de Termología, Facultad de Ciencias Universidad Autònoma de Barcelona, Bellaterra, Barcelona, Spain

The rate of crystallization of $(GeSe_2)_{70}(Sb_2Te_3)_{20}(GeTe)_{10}$ vitreous samples was investigated by means of differential scanning calorimetry. Crystallization proceeds in two stages. The activation energy of each stage of crystallization was determined. The evolution of the microstructure during crystallization was investigated by X-ray analysis and optical and scanning electron microscopy. Crystalline nuclei emerge in the bulk and develop in a spherulitic form. A lamellar structure is clearly observed when crystallization is completed.

1. Introduction

Glass formation is often observed in molten alloys formed from a variety of elements of differing valency. Such compositions favour a fully connected structure with all the bonds satisfied and this leads to a greater glass-forming tendency. Consequently, the glass-forming regions are expected to be considerably extended by the addition of a third or fourth component to a binary glass-forming system. In previous investigations [1, 2] it was shown that the addition of Sb_2Te_3 to alloys of the system $GeSe_2$–GeTe results in a wide region of glass formation. By water quenching it is possible, for instance, to prepare glasses with up to 30 mol% Sb_2Te_3. Probably melt units of general formula GeX_2 (X = Se, Te) and Y_2Se_3 (Y = Ge, Sb) are formed, favouring glass formation [3, 4].

Little is known about the nature of the crystallization process in these types of alloy glasses. One important well known feature is that crystallization is a highly exothermic process, and this makes differential scanning calorimetry (DSC) a very suitable technique for the study of the kinetics of the process. Furthermore, as these materials are good glass formers, their microstructure and growth characteristics can be recognized in the early stages of crystallization.

In this paper we report on the crystallization behaviour of a $(GeSe_2)_{70}(Sb_2Te_3)_{20}(GeTe)_{10}$ water-quenched glass. The determination of the temperatures and activation energies for each stage of crystallization has been derived from DSC results. The morphology of the crystallization reaction has been investigated using both scanning electron microscopy (SEM) on fresh fracture surfaces and metallographic observation of polished surfaces. The relation between the evolution of both the microstructure and the enthalpy changes during crystallization is discussed.

2. Experimental procedure

Bulk glassy samples were prepared by melting weighed amounts of the elements (5N purity) in evacuated and sealed quartz ampoules. The molten alloy was held at 1275 K for 12 h, constantly agitated to ensure homogeneity, and subsequently quenched to room temperature in water.

*Work supported by CAICYT. Project no. 0310.
‡Permanent Address: Física del Estado Sólido, Facultad de Física, Universidad de Barcelona, Diagonal 645, Barcelona-28, Spain.

0022–2461/83 $03.00 + .12

DSC experiments were carried out with a Perkin Elmer DSC-2 on about 10 to 15 mg of the investigated alloy. Measurements were carried according to the following methods: (a) constant heating rate experiments were recorded, from room temperature to beyond the crystallization exotherms, under a pure argon atmosphere at scan rates β ranging from 2.5 to 80 K min^{-1}. We followed the usual procedure [5] for calibrating the measured temperature and heat of transition with the melting point and latent heat of indium, tin, lead and zinc. (b) Isothermal measurements were performed by heating at a rate of 320 K min^{-1} until the annealing temperature was reached. The fraction α of material crystallized at a given time t was determined from the ratio between the subtended area at that time and the area of the complete exothermic peak. Similarly, the transformation rate $d\alpha/dt$ at a time t was determined by the ratio between the height of the DSC curve and the area of the complete transformation curve. This procedure is based on two assumptions. (i) The amount of transformation after continuous heating at 320 K min^{-1} from room temperature to the temperature T is negligible (as it would be on heating instantaneously to T). (ii) The temperature of the liquid–solid interface is not affected by the liberation of the latent heat of fusion at the growth interface during the crystallization process. The first assumption limits the upper temperature at which isothermal annealing could be analysed. The entropy of fusion for the alloy glass is about $1.4R$. Consequently the second assumption requires a maximum growth rate not exceeding 10 μm sec^{-1} [6].

Other samples were heat-treated in the calorimeter by scanning up to temperatures corresponding to characteristic points of previous DSC curves. The samples were finally quickly removed from the calorimeter and quenched to room temperature.

Microscopic observations were then made to identify the structural changes which were responsible for the thermal transitions observed in the DSC.

Metallographic examination on mechanical polished samples was performed using an Leitz Ortholux II Pol BK optical microscope. Scanning electron microscope observations of fresh fracture surfaces were made using either an ISI S-III A SEM or a Philips 500 SEM with energy dispersive X-ray analysis facilities. X-ray diffraction was carried out on a vertical goniometer using Cu$K\alpha$ radiation.

3. Differential scanning calorimetric results

The kinetic analysis of the crystallization process has been performed either by isothermal annealing or by heating at selected rates. Fig. 1 shows an example of the DSC curves obtained at a heating rate of 20 K min^{-1}. The inflection (a slight dip) prior to the first crystallization peak corresponds to the glass transition. The glass transition temperature, T_g, was defined as the temperature where the DSC curve showed an endothermic change of slope in the DSC trace. There are also two well-defined, though overlapped, exothermic peaks which will be labelled A and B. The enthalpies associated with the A and B peaks are 3.1 ± 0.3 and 2.0 ± 0.3 kJ mol^{-1}, respectively. Experimental values of T_g, and of the respective maximum peak temperatures T_{PA} and T_{PB} are summarized in Table I.

To explain the thermal behaviour on crystallization we assume that the rate of crystallization is given by

$$\frac{d\alpha}{dt} = k(T) f(\alpha) \qquad (1)$$

Here $f(\alpha)$ is a function which is related to the mechanism of crystallization and $k(T)$ is given by the Arrhenius expression

$$k(T) = k_0 \exp(-E/RT) \qquad (2)$$

where k_0 is a pre-exponential factor and E the effective activation energy [6–8].

For isothermal crystallization, a plot of ln $(d\alpha/dt)$ against $1/T$, at a fixed value of α but different isothermal annealing, should give a straight line of slope $-E/R$ and intersect ln $[k_0 f(\alpha)]$. If the transformation rate depends only on the state variables α and T, and not on thermal history,

TABLE I Glass transition values, T_g, and first, T_{PA}, and second, T_{PB}, crystallization peaks, for $(GeSe_2)_{70}(Sb_2Te_3)_{20}(GeTe)_{10}$ glasses as a function of the scanning rate β

β (K min^{-1})	T_g (K)	T_{PA} (K)	T_{PB} (K)
2.5	499.5	593.5	644.5
5	502	603.5	649
10	505	615	656
20	510	628	665
40	514	641	677
80	517	656	684

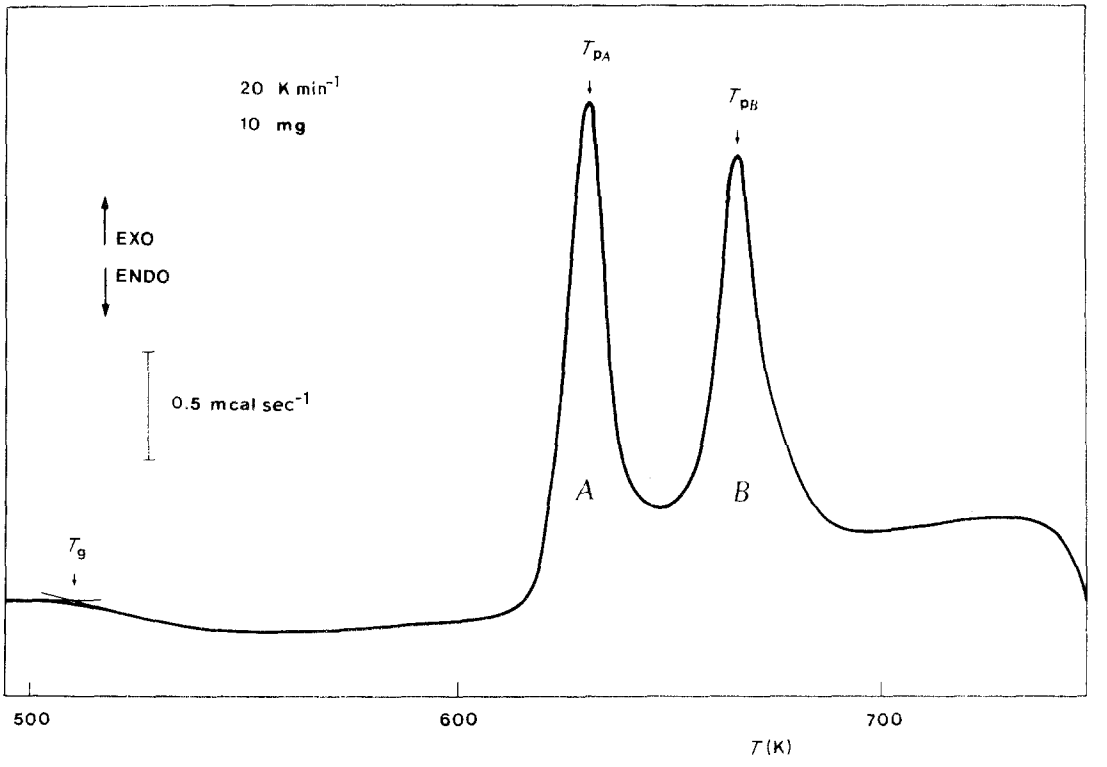

Figure 1 Typical DSC curve obtained at a heating rate of 20 K min^{-1}. Arrows indicate the glass transition temperature, T_g, and the crystallization peak temperatures T_{PA} and T_{PB}.

then for non-isothermal crystallization a plot of $\ln(d\alpha/dt)$ against $1/T$ should similarly show a linear behaviour with a slope also equal to $-E/R$.

A peak method has also been used to obtain the activation energy in non-isothermal measurements. It uses the fact that at the maximum peak temperatures, $(d^2\alpha/dt^2)_{T=T_p} = 0$ [9]. This condition can be rewritten in terms of the constant heating rate β and of the activation energy as:

$$\ln(\beta/T_p^2) = -E/RT_p + A \qquad (3)$$

where A is a smooth function of α though can be assumed to be constant for moderate values of β [10].

3.1. Isothermal annealing

Isothermal calorimetric data obtained for the peak A at temperatures of 595, 600, 605 and 610 K were analysed. The plots of $\ln(d\alpha/dt)$ against $1/T$ at a fixed α yield a straight line with a slope which is independent of α. We conclude that, in the temperature interval studied, an activation energy which is independent of both the temperature T and the transformed fraction α can be defined. A value for $E = (175 \pm 5)$ kJ mol^{-1} is obtained. Since it seems doubtful that both the nucleation and the crystalline growth rate would have the same temperature dependence, it appears more convenient to assign the observed activated energy to the crystalline growth rate rather than to the nucleation rate [11].

The analysis of $f(\alpha)$ in Equation 1 is useful to distinguish which one of the kinetic models can explain the results. This analysis is, however, only feasible when these kinetic models prove to be distinguishable under the given conditions, i.e. when their characteristic equations differ for each model represented in an appropriate coordinate system [12]. In order to perform this analysis and to decide which kinetic model agrees better with our experimental crystallization data, we compare the experimental dependence of $\ln[k_0 f(\alpha)]$ against $\ln(1-\alpha)$ and that predicted, assuming different model equations for $f(\alpha)$. Fig. 2 shows the kinetic model that gives the best fit to our experimental results. This model can be represented by the equation

$$f(\alpha) = n(1-\alpha)[-\ln(1-\alpha)]^{(n-1)/n} \qquad (4)$$

with $n = 2.4 \pm 0.2$, corresponding to a three-

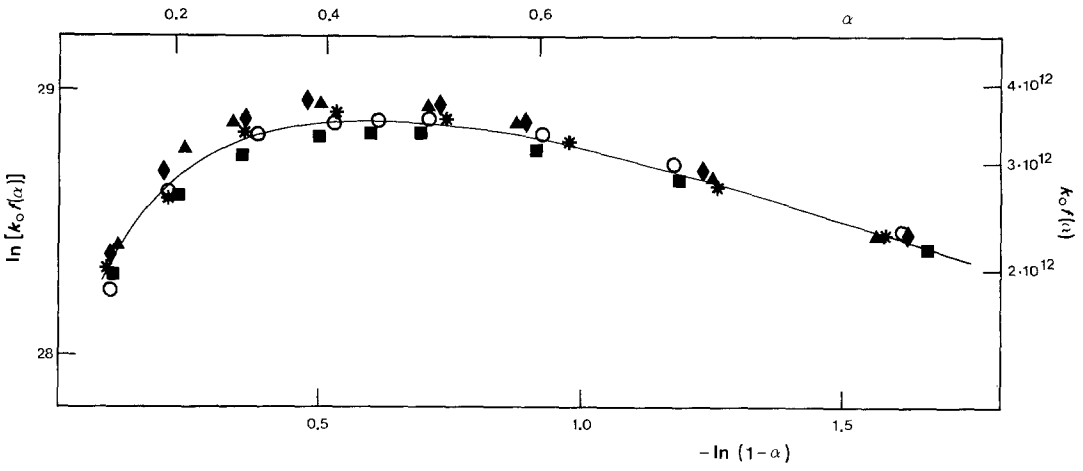

Figure 2 Plot of $\ln [k_0 f(\alpha)]$ against $\ln (1-\alpha)$ for $(GeSe_2)_{70}(Sb_2Te_3)_{20}(GeTe)_{10}$ glass. Experimental data obtained at (○) 595 K; (■, ∗) 600 K; (▲) 605 K and (♦) 610 K. (——) Theoretical curve obtained with Equation 2.

dimensional volume growth, controlled by diffusion [13]. A value of $k_0 \sim 3 \times 10^{12}$ sec is obtained.

3.2. Non-isothermal (constant heating rate) measurements

The activation energy of both peaks (A and B) has been measured from the temperature shifts obtained on heating at selected rates in the DSC. Fig. 3 shows the plots of $\ln (\beta/T_p^2)$ against $1/T_p$. This method offers the advantage of allowing the determination of the activation energy relevant to the second stage of crystallization (B peak) which cannot be obtained simply by isothermal measurements. The activation energies deduced are (168 ± 6) and (289 ± 8) kJ mol^{-1}, respectively for the A and B peaks. The agreement with the value obtained in isothermal measurement of peak A is, indeed, excellent, showing that thermal history in these experiments has a negligible effect on the activated process.

4. Structural analysis

The amorphous state of the water-quenched samples was demonstrated by X-ray diffraction. Their homogeneity was tested by light microscopy and in some cases by electron microscopy. No phase separation was observed. Fig. 4 shows the experimental wide angle X-ray diffraction patterns. The as-quenched sample, curve (a), consists of two diffuse halos centred at $(4\pi \sin\theta)/\lambda = 20.4$ and

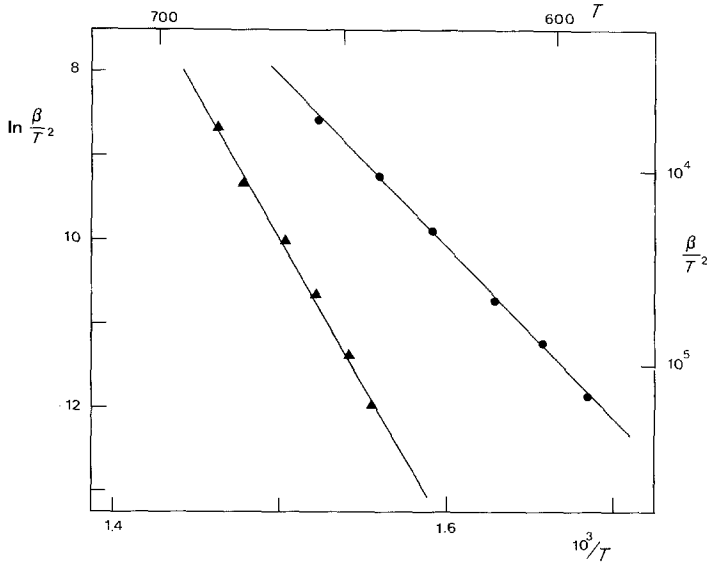

Figure 3 Kissinger plots of $\ln (\beta/T_p^2)$ against $1/T_p$ for the two crystallizations peaks of $(GeSe_2)_{70}(Sb_2Te_3)_{20}$-$(GeTe)_{10}$ glass. (●) A peak, (▲) B peak.

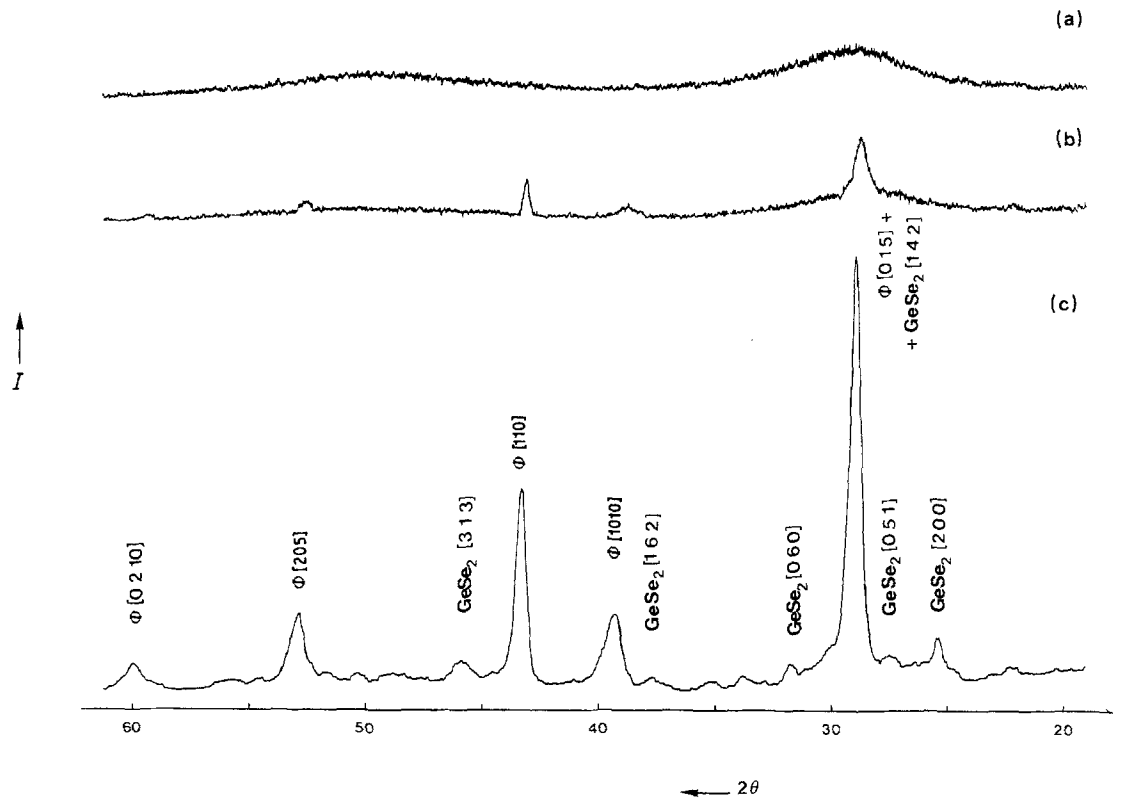

Figure 4 X-ray diffraction pattern for $(GeSe_2)_{70}(Sb_2Te_3)_{20}(GeTe)_{10}$ samples (Cu$K\alpha$ line is used) (a) as-quenched, (b) after the onset of the first crystallization peak, (c) after complete devitrification. Abcissa represents 2θ and ordinate the diffracted intensity I in arbitrary units.

$34.3\,nm^{-1}$ showing the amorphous character of the samples. The spacings calculated from the first peak according to Ehrenfest's relation [14] is 0.385 nm. An identical diffractogram was obtained when the sample is previously heated at $5\,K\,min^{-1}$ to just over T_g and then cooled to room temperature. Curve (b) shows the pattern corresponding to a sample heated until the onset of peak A. Here distinguishable reflections are obtained, indicating the presence of an emerging crystalline phase. After complete devitrification curve (c) is found. This diffraction pattern shows the superimposition of reflections of at least two crystalline phases. One phase corresponds to $GeSe_2$ [15]. The second one is a new phase which we call ϕ. We know that there is a large solid solubility range in the $GeSe_2$–Sb_2Te_3 system [16] going from pure Sb_2Te_3 to 55 mol% $GeSe_2$, and that the hexagonal Sb_2Te_3 cell parameters decrease when $GeSe_2$ is added. From this we infer that the phase ϕ, which has also a hexagonal structure with lattice parameters slightly lower than those of Sb_2Te_3, is a ternary solid solution with a composition that is not exactly known. Comparison of curves (b) and (c) indicates that the crystallization tendency of the phase ϕ is greater than that of $GeSe_2$.

There is no significant difference between the X-ray diffraction pattern obtained from a sample quenched to room temperature from a temperature just above peak A, and that of curve (c) of Fig. 4. These results indicate that peak B does not involve any modification of the crystalline structure. The estimated size of the coherently diffracting domains for each crystalline phase is about 20 nm [14]. No paracrystalline lattice distortion [17] was observed.

5. Metallographic and scanning electron microscopy

Optical and scanning electron microscopy were employed to observe the type and the extent of crystallization obtained during the thermally activated devitrification of the glassy samples. The progress of crystallization is obtained by heating the bulk glassy samples from room temperature to some preselected temperatures in the

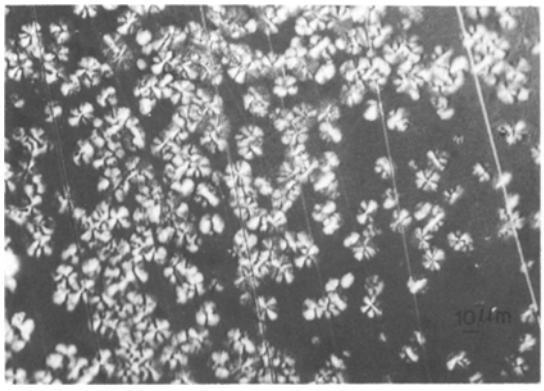

Figure 5 Optical micrograph under crossed polaroid showing the spherulitic growth of the alloy glass.

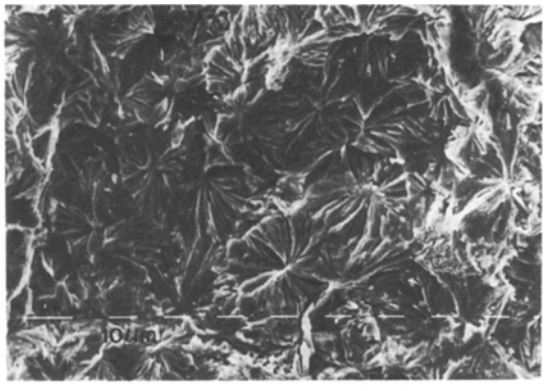

Figure 7 SEM micrograph showing the morphology of a sample heated above T_{PA} at 20 K min^{-1}.

DSC, and then cooling again to room temperature. These temperatures correspond to some of the characteristic features of the actual calorimetric DSC curves.

In samples heated just above T_g (Fig. 1) no development of crystallinity is observed. Once the onset of the A peak is reached the presence of some crystallites can be observed in the bulk. Their distribution is typically random. On further heating the spherulitic aggregate form of the crystallites is more readily apparent (Fig. 5). Occasionally a series of spherulites all grow with their origins nucleated on a common line as shown in Fig. 6. After the first exothermic peak a coalescence of spherulites is obtained (Fig. 7). After the second exothermic transformation (peak B) no significant changes in the morphology occur. This result is consistent with the X-ray diffraction data obtained. The spherulites exhibit a conspicuous lamellar structure as shown in Fig. 8. It is worth noting the thickening of lamellae along the radius of the spherulite. The lamellae possess typical thicknesses ranging from 0.2 to 1.0 μm. In Fig. 9 a series of scanning electron micrographs showing the growth of spherulites in isothermal annealing are presented. Annealings ranging from 6 to 20 min at a temperature of 590 K have been performed and the size of the spherulites measured in each case. A crystal growth rate $u = 1.83 \times 10^{-8}$ m sec^{-1} has been deduced for the first stage of crystallization at that temperature. Furthermore, energy dispersive analysis has been done on partially crystallized samples. Within the spatial resolution limits in EDAX analysis, there is no concentration difference between the emerging spherulites and the vitreous matrix.

6. Conclusions

The coupling of both morphological and calori-

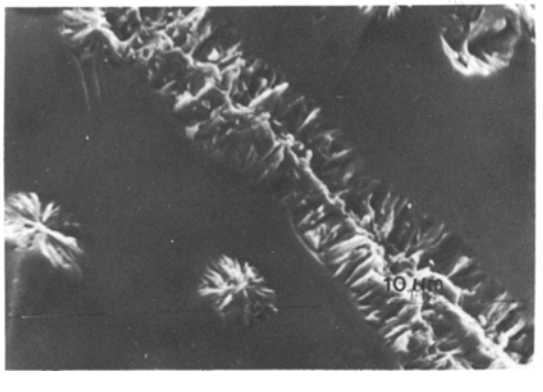

Figure 6 SEM micrograph of a fresh fracture after initial devitrification.

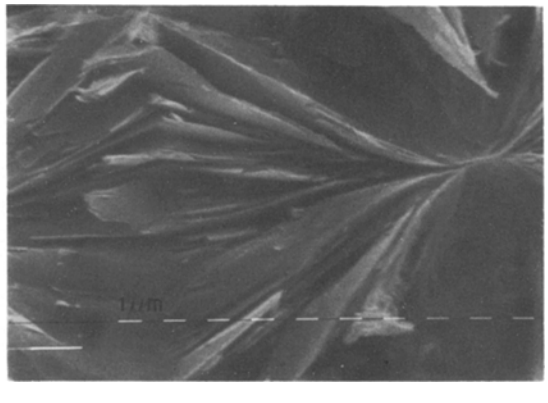

Figure 8 Lamellar structure of the sample after complete devitrification as shown by SEM.

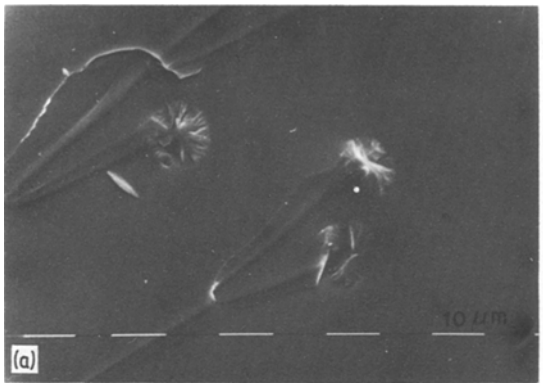

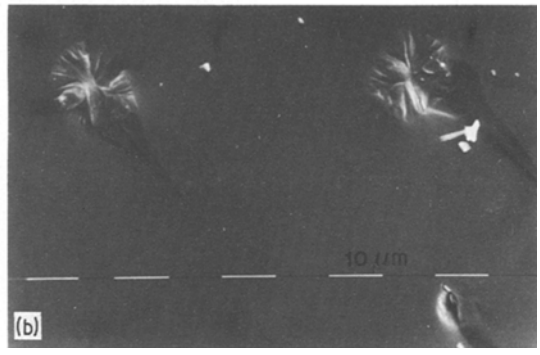

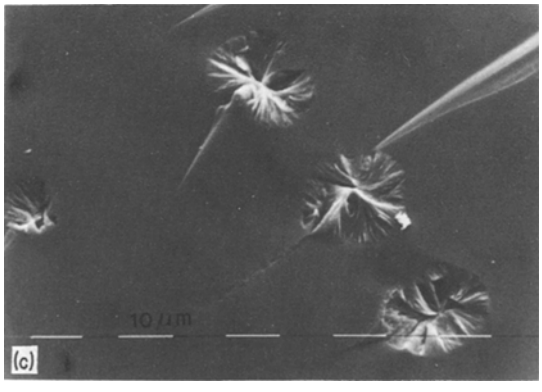

Figure 9 Progress of isothermal crystallization at 590 K. SEM micrographs for annealing times of: (a) 12 min; (b) 15 min; (c) 18 min.

metric studies has proved very useful in elucidating some of the factors controlling the crystallization process of $(GeSe_2)_{70}(Sb_2Te_3)_{20}(GeTe)_{10}$ alloy glasses. Calorimetrically this material shows a two-stage crystallization reaction with some overlapping of the exothermic peaks in DSC heating curves.

The contributions to the crystallization enthalpy from each stage of the process have been distinguished by DSC measurements in both isothermal and nonisothermal conditions. Crystalline nuclei develop into spherulites. No evidence for a preferential surface nucleation is obtained.

The crystallization process begins at the onset of the first exothermic peak and is completed once this first peak is ended. The crystallized sample consists of two phases: $GeSe_2$ and a solid solution which we call phase ϕ. The enthalpy of the second peak is slightly lower than that of the first one. However, during the second exothermic stage of crystallization neither morphological nor crystalline modifications of the sample are detected. Further studies are necessary for a better understanding of the second stage of crystallization.

The spherulites have a lamellar radial structure with some large interlamellar empty regions. From the comparison of the thickness of the lamellae and the broadening of the diffraction lines of the crystalline phases it is suggested that although phase ϕ has a larger crystallization driving force than $GeSe_2$, once the reaction is initiated it proceeds as a lamellar eutectic crystallization in which long range diffusion is necessary for the redistribution of the components into the two phases.

Acknowledgements

The authors wish to thank Dr A. Traveria for X-ray diffractogram measurements, Dr A. Alvarez for preparing the polished samples, and Ms M. Marsal for her skills in SEM and EDAX analysis. They are also indebted to Professor F. J. Baltá-Calleja for valuable and encouraging discussions and critical reading of the manuscript.

References

1. S. SURIÑACH, M. D. BARO, M. T. CLAVAGUERA-MORA and N. CLAVAGUERA, Proceedings of "Chemistry and physics of sulfides, selenides and tellurides in solids", edited by J. Flahaut, Paris, September 1981, Poster J.9.
2. S. SURIÑACH, M. D. BARO, M. T. CLAVAGUERA-MORA and N. CLAVAGUERA, Proceedings of 7th ICTA, Ontario, August 1982, edited by B. Miller (Wiley, 1982) p. 127.
3. S. C. ROWLAND, S. NARASIMHAN and A. BIENESTOCK, *J. Appl. Phys.* **43** (1972) 2741.
4. G. LUCOVSKY, R. J. NEMANICH and F. L. GALEENER, Proceedings of 7th International Conference on Amorphous and Liquid Semiconductors, Dundee, 1977, edited by W. E. Spear (University Edinburgh, Edinburgh 1977) p. 130.
5. G. LOMBARDI, "For Better Thermal Analysis", edited by ICTA Roma (1980) p. 28.

6. D. W. HENDERSON, *J. Non-Cryst. Solids* **30** (1979) 301.
7. J. SESTAK and G. BERGGREN, *Thermochim. Acta* **3** (1971) 1.
8. H. S. CHEN, *J. Non-Cryst. Solids* **27** (1978) 257.
9. H. E. KISSINGER, *Anal. Chem.* **29** (1957) 1702.
10. M. D. BARO, N. CLAVAGUERA, S. BORDAS, M. T. CLAVAGUERA-MORA and J. CASAS-VAZQUEZ, *J. Thermal Anal.* **11** (1977) 271.
11. D. G. MORRIS, *Acta Metall.* **29** (1981) 1213.
12. J. PLEWA, J. NORWISZ, N. HAJDUK and M. ROMANSKA, *Thermochim. Acta* **46** (1981) 217.
13. J. SESTAK, Proceedings of the 3rd ICTA, Vol. 2, edited by H. G. Wiedamann (Birkhäuser Verlag, Basel, 1972) p. 3.
14. A. GUINIER, "Théorie et Technique de la Radiocristallographie" (Dunod, Paris, 1964).
15. G. D. DITTMAR and H. SCHAFER, *Acta Cryst.* **B32** (1976) 2726.
16. S. SURIÑACH, Masters thesis, Universidad Autónoma de Barcelona (1979).
17. R. HOSEMANN and S. N. BAGCHI, "Direct Analysis of Diffraction by Matter" (North-Holland, Amsterdam, 1962).

Received 12 July
and accepted 4 October 1982